SECURITY CLASSIFICATION OF THIS PAGE

REPORT DOCUMENTATION PAGE

1a. REPORT SECURITY CLASSIFICATION UNCLASSIFIED	1b. RESTRICTIVE MARKINGS
2a. SECURITY CLASSIFICATION AUTHORITY	3. DISTRIBUTION/AVAILABILITY OF REPORT Approved for public release, distribution unlimited.
2b. DECLASSIFICATION/DOWNGRADING SCHEDULE	
4. PERFORMING ORGANIZATION REPORT NUMBER(S) NRL Report 9022	5. MONITORING ORGANIZATION REPORT NUMBER(S)
6a. NAME OF PERFORMING ORGANIZATION Naval Research Laboratory 6b. OFFICE SYMBOL (*If applicable*) Code 5110	7a. NAME OF MONITORING ORGANIZATION
6c. ADDRESS (*City, State, and ZIP Code*) Washington, DC 20375-5000	7b. ADDRESS (*City, State, and ZIP Code*)
8a. NAME OF FUNDING/SPONSORING ORGANIZATION Office of Naval Research 8b. OFFICE SYMBOL (*If applicable*)	9. PROCUREMENT INSTRUMENT IDENTIFICATION NUMBER
8c. ADDRESS (*City, State, and ZIP Code*) Arlington, VA 22217	10. SOURCE OF FUNDING NUMBERS PROGRAM ELEMENT NO. 61153N 32 / PROJECT NO. RR032 0141 / TASK NO. / WORK UNIT ACCESSION NO. DN180-028

11. TITLE (*Include Security Classification*)
Characteristics of the Two-Dimensional Spectrum of Roughness on a Seamount

12. PERSONAL AUTHOR(S)
Czarnecki, M. F. and Bergin, J. M.

13a. TYPE OF REPORT	13b. TIME COVERED	14. DATE OF REPORT (*Year, Month, Day*)	15. PAGE COUNT
Interim	FROM 10/84 TO 10/85	1986 December 23	26

16. SUPPLEMENTARY NOTATION

17. COSATI CODES			18. SUBJECT TERMS (*Continue on reverse if necessary and identify by block number*)
FIELD	GROUP	SUB-GROUP	Ocean bottom roughness; Acoustic scattering; Two-dimensional spectra; Acoustic transmission loss; Seamount roughness; Multibeam bathymetric data

19. ABSTRACT (*Continue on reverse if necessary and identify by block number*)

Advances in bottom mapping technology, such as multibeam bathymetric survey systems, have made it possible to obtain detailed depth measurements over two horizontal dimensions and to develop statistical models that describe variability of small-scale ocean bottom roughness. This report investigates the nature of the two-dimensional power spectrum of the bottom roughness on a seamount. The characteristics of the power spectra are discussed; particular emphasis is placed on the issues of anisotropy and the power law behavior of the bottom roughness.

20 DISTRIBUTION/AVAILABILITY OF ABSTRACT	21. ABSTRACT SECURITY CLASSIFICATION
☒ UNCLASSIFIED/UNLIMITED ☐ SAME AS RPT. ☐ DTIC USERS	UNCLASSIFIED
22a NAME OF RESPONSIBLE INDIVIDUAL Michael F. Czarnecki	22b. TELEPHONE (*Include Area Code*) (202) 767-3013 22c. OFFICE SYMBOL Code 5110

DD FORM 1473, 84 MAR 83 APR edition may be used until exhausted. All other editions are obsolete

SECURITY CLASSIFICATION OF THIS PAGE

☆U.S. Government Printing Office: 1985–507-047

Naval Research Laboratory
Washington, DC 20375-5000 NRL Report 9022 December 23, 1986

Characteristics of the Two-Dimensional Spectrum of Roughness on a Seamount

MICHAEL F. CZARNECKI AND JOHN M. BERGIN

Acoustics Media Characterization Branch
Acoustics Division

CONTENTS

CHARACTERISTICS OF THE TWO-DIMENSIONAL SPECTRUM OF ROUGHNESS ON A SEAMOUNT

INTRODUCTION

The seafloor has a wide variety of topographic features. The lateral extent of these features ranges over at least nine orders of magnitude, from a fraction of a centimeter to thousands of kilometers. Vertical relief similarly varies over a comparable range from millimeters to several kilometers. The long and intermediate scale features such as ridges, continental slopes, abyssal plains, fracture zones, trenches, and seamount chains are reasonably well defined as a result of historical bathymetric surveys. Until recently, however, very little detailed quantitative information has been available on smaller scale seafloor variability less than several kilometers in spatial extent. Advances in bottom mapping system technology, such as the Sonar Array Sounding System (SASS) and Sea Beam, have made it possible to obtain detailed depth measurements over two horizontal dimensions.

A real challenge presented by such detailed measurements is to develop convenient techniques for characterizing the complex variability that lend themselves to further geological studies. Statistical methods offer one approach to the general problem, especially the theory of stochastic processes whereby the ocean bottom is regarded as a random process that evolves as a function of two spatial coordinates. A further motivation for the development of statistical models of bottom variability comes from modern theories of oceanic processes, which often require statistical descriptions of ocean bottom roughness.

We here investigate the nature of the two-dimensional (2-D) power spectrum of the bottom roughness on Apuupuu seamount, which is located 130 km south of Hawaii. Apuupuu seamount was chosen because of the existence of fairly complete data coverage by multibeam measurements. The power spectral density is a useful representation of bottom roughness because it describes the distribution of mean-square residual elevation among the spectral components, i.e., as a function of wavelength. In the 2-D context, it preserves the directional attributes of the bottom topography. Further, the 2-D spectrum (or the correlation function, through a Fourier transform relation) plays a basic role in the characterization of the bottom roughness as a stochastic process. Bottom roughness means topographic variability with horizontal spatial scales shorter than 1600 m. This scale length is partly determined by the nature of the data but, more significantly, is a length small in comparison to the overall lateral dimension of the seamount.

Previous efforts to describe the spectral content of the ocean bottom variability have been limited in number and usually restricted to 1-D representations derived from single-beam bathymetric tracks. Neidell (1966) generated power spectra from bathymetric, magnetic, and gravimetric data collected in the Atlantic and Indian oceans. He noted that the spectra were "red" in nature in that they characteristically exhibited a decrease in power with increasing wavenumber. Bell (1975) presented a functional relationship for the 1-D spectrum of abyssal hill topography. Most recently, Berkson and Matthews (1984) generated 1-D spectral estimates for a wide range of bottom regimes and noted that they exhibited spectral slopes from -1 to -5, suggesting that a power law behavior generally applies to ocean bottom spectra. The existence of a power law behavior is also found for other rough surfaces. For example, Frederiksen and Jacobi (1981) found similar power laws for terrestrial topography and have used the spectral slope to classify types of terrain. Brown and Scholz (1984) established that rock surfaces also exhibit a red-noise spectrum over a wavelength band extending from 20 μm to $\sim$1 m, with

Manuscript approved September 9, 1986.

the power falling off between 2 and 3 orders of magnitude per decade increase in spatial frequency. An implication of these 1-D results is that while a power-law behavior may be expected, the spectral description will be dependent on the nature of the physiographic regime.

The topography of a seamount was selected for study here because it allows the investigation of a member of a single physiographic regime in great detail. Evaluation of the 2-D spectrum allows discussion of several issues that do not arise in the spectral analysis of processes that depend on only one independent variable. A particular aspect of great interest involves the anisotropy of the bottom roughness, or the need to refer the 2-D spectral representation to a reference direction. The question of anisotropy is particularly relevant for seamounts since there are obvious "special directions" (such as downslope) for the large-scale aspects of the seamount. It is also a question of fundamental importance to the interpretation and proper use of single-track bathymetry. Bell (1979), in extending his previous work, stressed the generally anisotropic nature of the seafloor. He suggested that a complete spectral description of the seafloor must be two-dimensional. Some earlier, but limited, efforts to study the azimuthal variation of bottom roughness included the work of MacDonald and Katz (1969), who generated polar autocorrelation functions and Akal and Hovem (1978), who computed 2-D power spectra from stereo bottom photographs. It is only recently that multibeam bathymetric survey systems have provided the sufficiently detailed bathymetric data sets that make feasible the investigation of bottom variability through 2-D spectral techniques. Included in this report is a description of the data set, signal processing procedures, and the resulting 2-D spectra for the Apuupuu Seamount.

MULTIBEAM BATHYMETRIC MEASUREMENT SYSTEM

Multibeam sonar systems represent one of the best available means for precision mapping of wide areas of the seafloor and consequently of providing quantitative information on seafloor topography. The concept of multibeam echo sounding by electronic array stabilization techniques was presented by Tucker and Henderson (1961). Several commercial sonars using this technology have been developed for various applications. The data used in this study were generated by the Sonar Array Sounding System (SASS) developed for the U.S. Naval Oceanographic Office. Glenn (1970) gives an introduction to this system, and data collected with this system were reported by Phillips and Fleming (1977) in a study of the Mid-Atlantic Ridge.

Multibeam bathymetric mapping systems are different from conventional echo sounders. Instead of a single, unstabilized beam of up to 60° in solid angle, the multibeam system uses a series of 61 roll and pitch-stabilized narrow beams of ~1.5° (Fig. 1). This technique provides a narrow fan of sound transverse to the ship's track that sweeps out a swath on the seafloor as the survey ship moves along its track. This sonar beam structure is the result of the composite of beam patterns of separate hull-mounted orthogonal arrays of sonar projectors and hydrophones. The vertical orientation of the arrays is electronically simulated by using attitude information provided by the ship's MK 3 SINS inertial navigation system. Pitch is stabilized by phase shifting the 12 kHz cw output pulses to the along-keel sonar projectors. The reflected acoustic signals returning from the seafloor are received by the transverse hydrophone elements and are processed into beams by beamforming techniques. The beams are compensated for ship's roll, and the received signals are digitized for input to the onboard computer. The depth for each of the sonar beams is calculated by using corrections for ship's pitch, roll, heading, and for vertical ray bending based on the measured sound velocity gradient structure.

Each output pulse of the sonar projector results in an array of up to 61 discrete depth points that are normal to the ship's track and cover a horizontal distance approximately equal to the depth of the water. The cross-track spacing of the depth points is a function of the depth of the water. It varies typically from the order of 25 m in 1500 m of water to 100 m for 5000 m of water. The along-track spacing is a function of survey vessel speed and projector pulse repetition rate. Typical survey speeds of 16 knots and ping intervals of 12 s result in the seafloor being ensonified by a fan of sound once every 100 m along the ship's track. Figure 2 is a typical plot of relative sonar beam positions for a number of data swaths collected over a seamount. Note in Fig. 2 that as the survey vessel travels over the summit of the seamount (located approximately in the center of the swath), the swath width varies from ~4 km

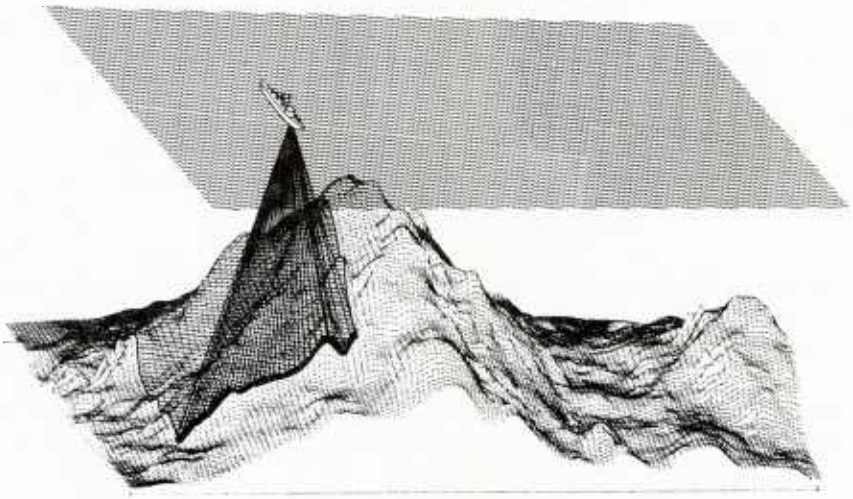

Fig. 1 — Schematic illustration of a swath on the ocean bottom sampled by a multibeam system

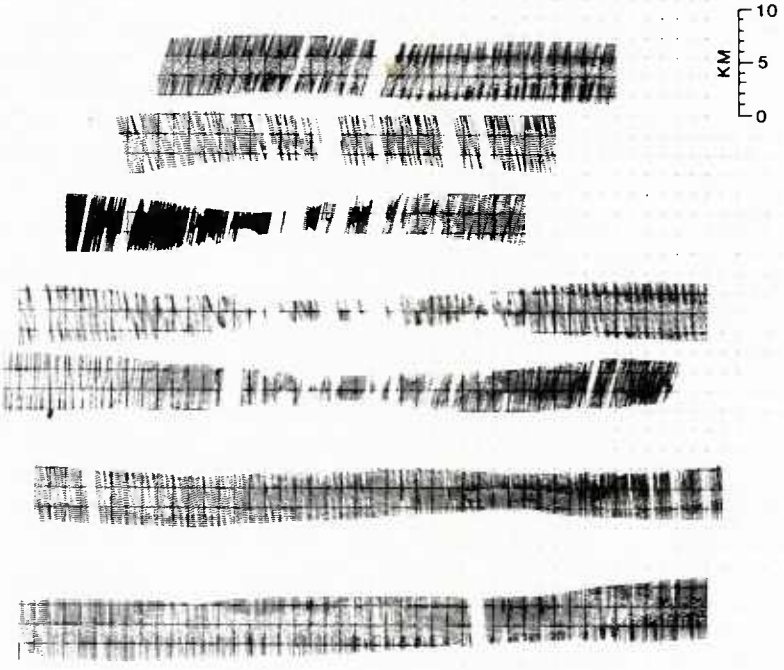

Fig. 2 — Typical multibeam sonar swaths over the summit of a seamount

in deeper water to 2.2 km at the summit and the cross-track spacing is not uniform. Raw data from the multibeam system takes the form then of a nonuniformly spaced series of depth values for each projector output pulse. The location of each individual beam is known relative to the ship's position at the time of the pulse. This location must be merged off-line with navigation data to produce bathymetry as a function of latitude and longitude. The system does have, however, the capability to adaptively correct in realtime for ship's velocity (as supplied by the SINS system) to provide a time-based contour chart of the bathymetric data on a true-distance scale. This feature allows an "instantaneous" look at the topography being surveyed and allows for on-site adjustment of the survey pattern, if necessary.

The line spacing of routine surveys performed to date has typically been on the order of 3 to 5 nmi. It has not, in general, produced overlapping swath data, except in areas where the water is very deep and the resulting swath width is large. Preliminary investigation of the data available from existing swaths that do overlap indicates that navigation mismatch between adjacent swaths preclude the direct use of combined bathymetry from overlapping swaths without time-consuming registration efforts. Bottom roughness investigations that require a true spatial representation of the bottom, such as the one described here, must for the present confine analysis to individual swaths. Recent use of the new satellite-based global positioning system (GPS) for navigation input has, however, produced excellent preliminary results and should produce significant reduction in position "mismatch" error for overlapping swaths in future surveys.

MULTIBEAM DATA PROCESSING

The seamount selected for this study is Apuupuu, which is located ~130 km off the southern coast of the island of Hawaii. Apuupuu is a good choice for a study of bathymetric roughness because it has an unusually thorough coverage by multibeam measurements. Before selecting sample patches of the bottom topography for statistical investigation, it is useful to use the entire mulibeam data set to construct an overall view of the shape of the seamount. The entire data set for Apuupuu consists of ~250,000 depth values. This is unnecessarily large for generating a large scale view of the seamount. Consequently, a decimated data set of ~10,000 depth values is obtained from the multibeam data set by using only data points that are spaced more than 500 m apart. These data are then contoured at vertical increments of 200 m (Fig. 3). Various perspective views are also generated to get an impression of the 3-D character of the seamount (Fig. 4).

Apuupuu covers an area of ~30 × 30 km and rises from a base depth of 4800 m to a summit at 2000 m. It is typical of many seamounts that even in large-scale relief they are not readily describable as simple geometric shapes. The large-scale relief is a result of complex geological mechanisms responsible for the formation of the seamount. One characteristic of Apuupuu is the presence of ridge-like structures that radiate outward from the main summit region. This structural pattern is associated with many seamounts. Vogt and Smoot (1984) have suggested that as seamounts evolve in time through several volcanic episodes they change from relatively axisymmetric structures to a star-shaped structure with these significant ridge complexes. The large-scale nature of the seamount proves important for the discussion of bottom variability.

Figure 5 is a block diagram of the data processing procedure used in this study to generate 2-D power spectral density estimates of the seamount bottom topography. A discussion of the essential aspects of the processing steps is included for completeness. It also points out the types of considerations that enter into the calculation of the 2-D power spectra.

Selection of Data Samples

Identification of a segment of data for 2-D power spectral density analysis involves a number of considerations including uniformity of data coverage, validity of the data, and the selection of signal processing techniques to be used. In this study, an area 1600 × 1600 m was selected as the bottom patch size for analysis, based on two criteria. First, the minimum swath width of the raw data available was ~2300 m. This set the upper limit on the practical size for a square patch that would fit within all

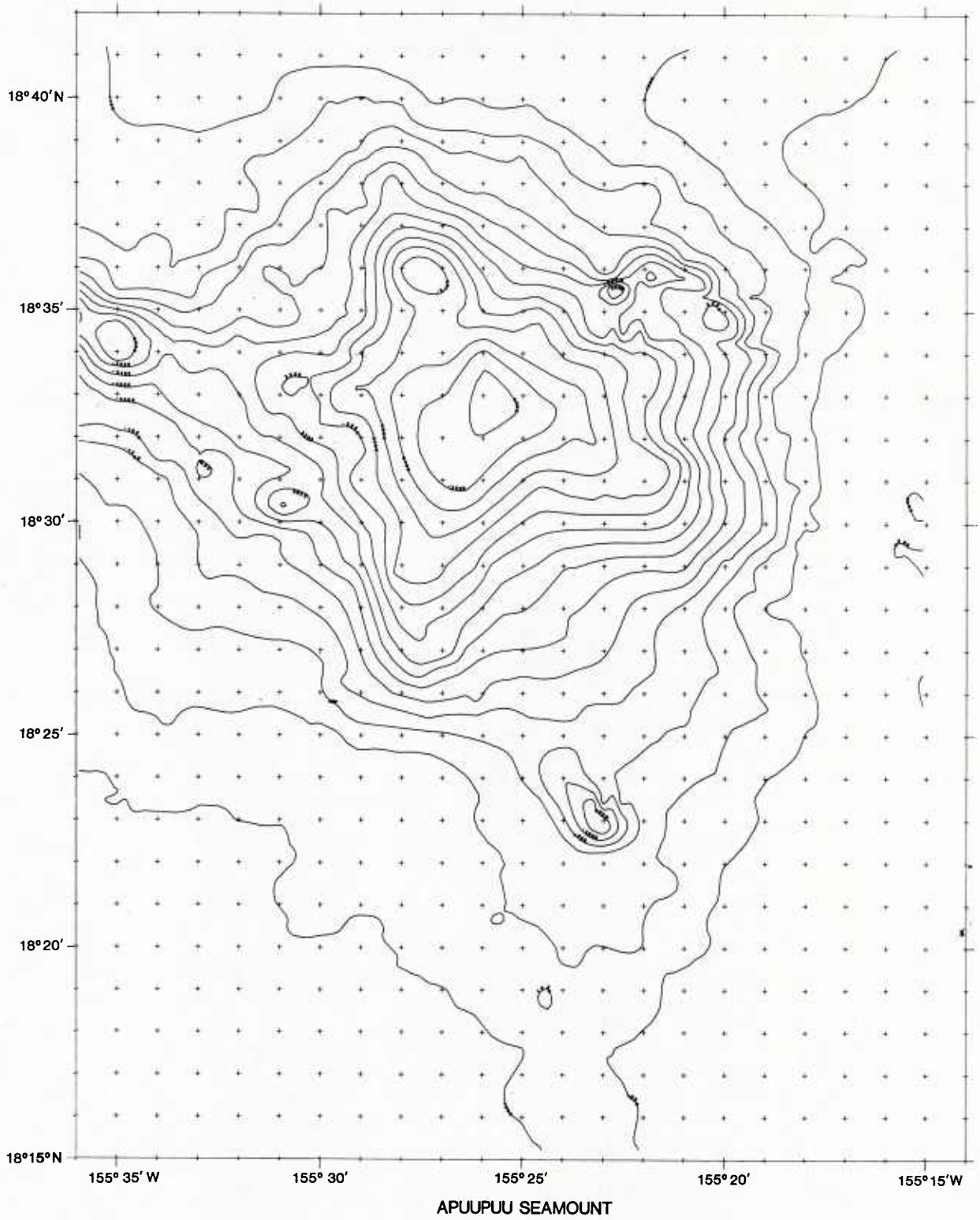

Fig. 3 — Bathymetric contours of Apuupuu Seamount

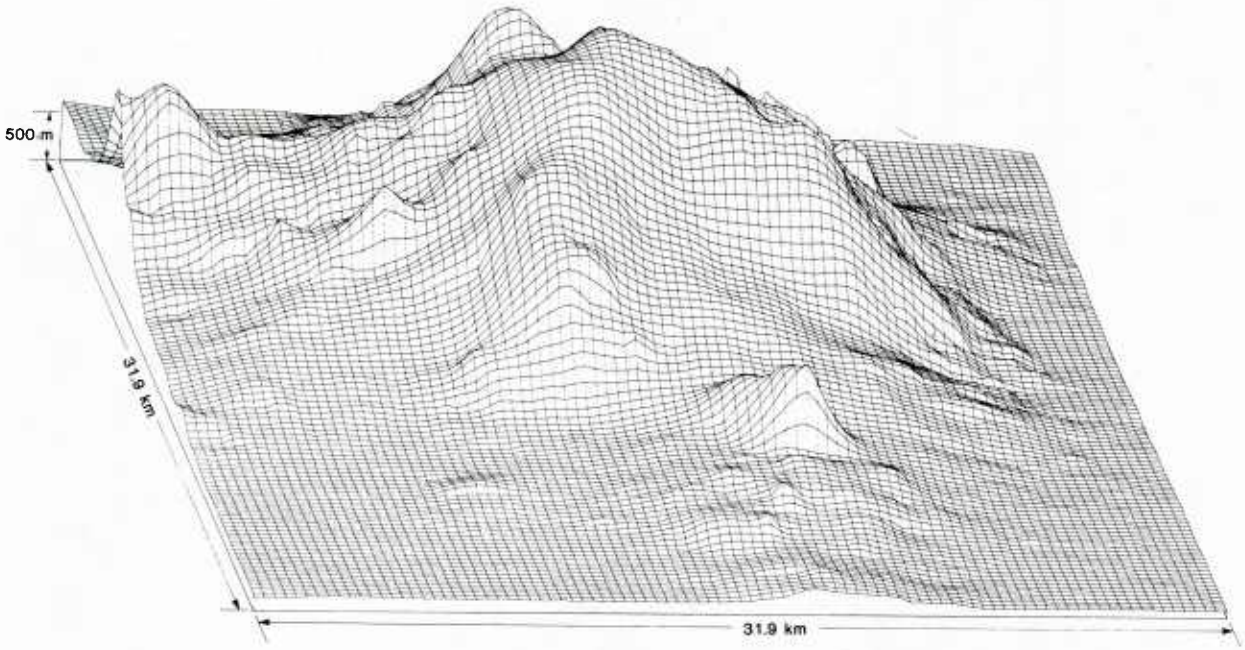

Fig. 4 — Large-scale structure of the Apuupuu Seamount is revealed by this perspective view from the south

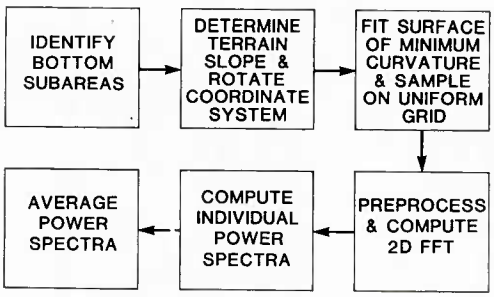

Fig. 5 — Block diagram showing the several steps required in the data processing of multibeam sonar data to produce power spectra for residual bathymetric surfaces

swaths. It was necessary to restrict the analysis to data within swaths to avoid the problem of navigation mismatch. This mismatch produces significant errors when investigating small scale bathymetric features. Second, a spatial sampling interval of at least 25 m was desirable to adequately represent the detailed cross-track structure of the multibeam data. The selection of a 25-m uniform sampling grid in conjunction with the 64 × 64 point 2-D power spectral density algorithm resulted in the 1600-m dimension for the square areas. The practice in this study was to initially work with areas the square root of two larger than 1600 m, i.e., square areas of 2260 m. Within this area, data coverage is relatively uniform and located close enough to the swath center to avoid ping-to-ping overlap of outer beams, a problem that occurs because of ship's yaw in higher sea states. Limiting the location of the study areas to the center of the swath also confines the data to a region where the uncertainty in the depth measurement is <5 m (rms). The reason for initially working with the larger areas is to allow for a variable orientation of the smaller 1600-m areas (hereafter referred to as subareas) that will be used in the spectral analysis.

The issue of orientation of data samples arises naturally for processes that depend on more than one variable. This is because one must, in general, allow for a statistical structure that is dependent on

direction. In particular, the 2-D spectrum of the process may be anisotropic, and, consequently, the procedure by which an estimate of the spectrum is calculated must account for any possible anisotropy. In some cases, the direction may be suggested by known physical aspects of the process. A good example is that of wind waves when the direction of the wind is used as the natural orientation for the discussion of the associated 2-D spectrum (Kinsman, 1965). The choice of such a direction for the statistical study of ocean bottom topography cannot be made with the same reliance on knowledge of the physical mechanisms. This is a consequence of the complexity of bottom topography and a lack of detailed knowledge about the mechanisms responsible for the topographic variability. The direction of anisotropy, then, must be regarded as an intrinsic part of the problem. As for the situation with the topography on a seamount, some guidance can be taken from the nature of the large scale structure. First, a crude picture of a seamount as a conical shape rising from the ocean bottom suggests a prominent direction at each point on the surface, corresponding to the maximum downslope direction. We modify this somewhat by using, as a reference direction, the maximum downslope direction at each location of interest determined by a local plane that is fit to the measured topography by least-squares regression. The reason for this modification is that it allows for the existence of the large-scale ridge-like structures already commented on before. This choice is justified because gravity is expected to play a significant role in the formation of seamount topography, and the local maximum downslope direction represents the direction determined by the projection of the gravity vector on the local mean plane. This choice of a local orientation direction is also well-suited for a study of the dependence of short wavelength processes on the large scale structure of the seamount. This issue is discussed later in connection with the spectral analysis.

An example of a subarea that results from the preceding considerations is shown in Fig. 6, together with an expanded view of the beam positions from one of the multibeam swaths. The figure also shows the locations of the uniformly spaced grid points at which bottom depth values are estimated for spectral analysis (see later text). Note that the individual beam locations are not uniformly spaced and that the selected subarea is rotated with respect to the along-track direction of the swath in such a manner that the y-axis points in the maximum direction. Contours of the total bathymetry are provided at 25-m increments and show a general agreement with the maximum downslope direction determined by fitting a mean plane to the data.

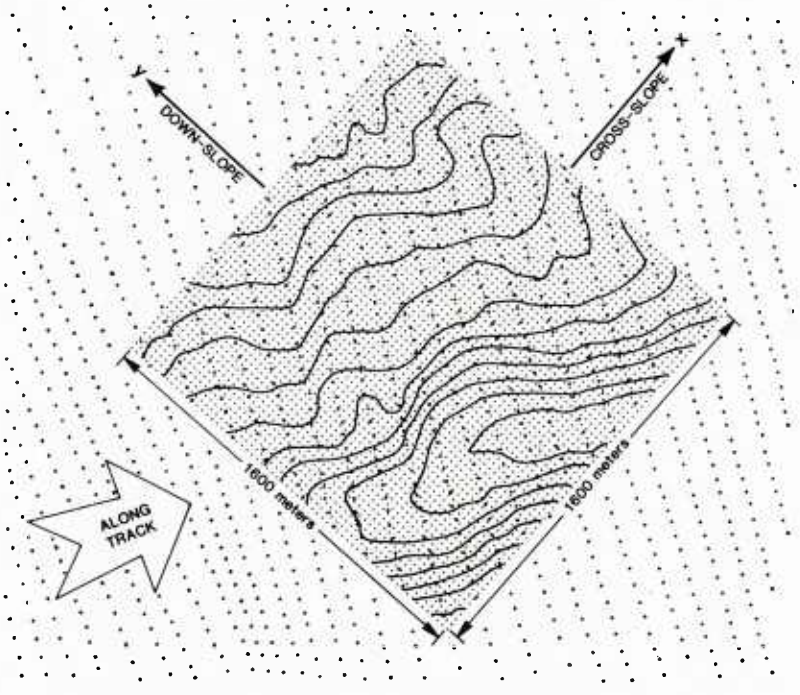

Fig. 6 — Expanded view of the beam positions for one of the multibeam swaths combined with the locations of the uniformly spaced grid and contours of the bottom topography

The multibeam swath data set for the Apuupuu Seamount yields 170 subareas, shown in Fig. 7, superimposed on 200-m bathymetric contours. This collection of samples of bottom topography from the seamount form the basic data set that will be used in the statistical study. The perceptible ordering of the subareas in the east-west direction arises from the original multibeam survey directions. The orientation of each subarea is indicated in this figure by an arrow indicating the local downslope coordinate system. It is clear from the figure that the distribution of the subareas over the region occupied by the seamount is fairly uniform. They also appear to offer an adequate sampling of most of the large scale features associated with the seamount.

Surface Fitting and Uniform Gridding

Using the two-dimensional fast Fourier transform (2D-FFT) for power spectral density (PSD) estimation requires that the data samples be located on a uniformly spaced grid. Consequently, the irregularly spaced multibeam sonar records must be resampled uniformly. This process is accomplished by fitting a surface of minimum curvature to the data by using the algorithm of Swain (1976). The surface of minimum curvature is constrained in this study to fit the original bathymetric data to within 1 m. The surface is then sampled on a rectangular grid with grid-point locations specified by the center of the subarea, the required coordinate system rotation, the desired x, y grid spacing, and the total number of x, y points. A brief discussion of the effects of resampling the data on the PSD calculation is warranted. The term resampling has been used because the sonar system has, in effect, already sampled the topography. Sampling theory defines the upper limiting wavenumber for spectral estimation to be given by the Nyquist rate

$$k_{MAX} = \left[2(\text{SAMPLING INTERVAL})\right]^{-1}, \tag{1}$$

where k_{MAX} is the highest wavenumber component of the spectra. For sampling a process that is dependent on two spatial variables, Eq. (1) applies to both sampling directions. The spectral content of the stochastic process being sampled that exceeds k_{MAX} "folds" around k_{MAX}, contaminating the spectral estimate by appearing as aliased energy at lower wavenumbers. For the seamount data of this study, the minimum cross-track and along-track raw data point spacings are ~25 m and 100 m, respectively. These correspond to maximum wavenumbers of 0.02 cycles/m and 0.005 cycles/m. Resampling this minimum curvature surface on a 25-m uniform grid then provides sufficient wavenumber coverage of calculated power spectra to be consistent with the maximum wavenumber expected in the data. Sampling on this grid, however, produces oversampling by a factor of 4 in the along-track direction. As a result, the surface of minimum curvature has been sampled or oversampled by a factor that ranges from slightly greater than 1 to 4, depending on the direction of resampling. Remember in subsequent analyses that the resulting data set is, as a result, a mixture of adequately sampled and oversampled data. This fact also means that the resampled data set is aliased differently as a function of direction, i.e., the cross-track data is potentially more affected by aliasing because it is sampled at a rate closer to its Nyquist rate. In all cases, however, aliasing by wavenumber content greater than $k_{MAX} = 0.02$ cycles/m is considered minimal because of the "red" nature of the spectra that causes the energy to fall off rapidly with increasing wavenumber.

One final caution must be stated in regard to resampling the multibeam data. Oversampling of the surface of minimum curvature fit to the multibeam sonar data does not increase the wavenumber content of the spectral estimate. Some distortion is possible if the surface "relaxes" between raw data points, but the minimum curvature aspect of the algorithm used significantly reduces this effect, and the spectral content is assumed to be essentially unchanged from the original samples. Interpretation of the resulting 2-D power spectra must be tempered by knowledge that the high wavenumber content in the along-track directing is limited to 0.005 cycle/m. Rotating the grid orientation to achieve the coordinate system where the Y-axis is downslope further complicates this interpretation because it is not readily apparent which direction is along-track. As a result, one must be cautious in extrapolating results beyond ~0.005 cycles/m With this criteria, the spectra are valid in all directions for wavelengths on the order of the subarea size, 1600 m down to ~200 m.

Preprocessing

Preprocessing the data prior to Fourier transformation is done in two stages. The first stage involves the removal of a least-squares plane from the data to produce a data set with zero mean and to remove any long wavelength trends. The result of this process is a residual bathymetric surface representing the random variations of the bathymetry. The second stage is the application of a 2-D Hanning window to the data. Windowing of the data is necessary because of the adoption of the Welch (1967) procedure by which statistically significant power spectral density estimates are determined by averaging spectra calculated from finite records or, in this case, finite patches of bathymetry. Selection of a finite patch size for spectral analysis, in effect, results in contamination of adjacent spectral components. This contamination results from "leakage" of sidelobes generated by the spatial domain convolution of the spectral content of the data with the Fourier transform of a uniform window equal to the extent of the finite patch. This contamination can be reduced significantly by using certain window functions that have specific characteristics. A thorough discussion of window functions and their characteristics is beyond the scope of this report; for details the reader is referred to a paper by Harris (1978). Two important parameters are the highest levels of the first sidelobe and the sidelobe fall-off rate. For any process, it is important that the first sidelobe of the Fourier transform of the window function be down significantly from the main spectral lobe to reduce the amount of energy leaked to adjacent components. In a "red noise-like" process, it is also important for the roll-off rate of the sidelobes to be greater than that of the process so that the window roll-off does not mask the roll-off of the process. Thomson et al. (1976) discuss this latter point. In the present study, spectral slopes potentially as great as -40 to -50 dB per decade of wavenumber are expected from the results cited by Berkson and Matthews (1984). Consequently, a 2-D cosine taper window of the form

$$W(r) = \cos^n (r) \tag{2}$$

is applied to the data, with r equal to the radial distance from the center of the subarea and n equal to 2. Under these conditions, this corresponds to a 2-D Hanning window that has a first sidelobe that is 32 dB down from the mainlobe and a roll-off rate of 60 dB per decade of wavenumber. Selection of this window provides the necessary sidelobe supression and roll-off for analysis of the bathymetric data. As with all windows, some broadening of the main lobe (a factor of 1.4 in this case) occurs, but the high roll-off rate of the Hanning window more than compensates for the reduced spectral resolution. It is more important to accurately estimate spectral slope characteristics than to resolve closely spaced spectral components.

Calculation of the Power Spectral Density

The 2-D fast Fourier transform (2D-FFT) used in this study is that of Robinson and Silvia (1981). The algorithm uses the fact that the 2D-FFT can be calculated by using a standard 1D-FFT algorithm to transform the data in one direction and then transforming the resulting matrix along the other axis. In this study, the matrix of 64 × 64 real values of residual bathymetry, i.e., bathymetry with a mean plane removed, is input to the algorithm. A 64-point complex 1D-FFT is applied to each of the columns of the matrix, and the results are stored in a temporary array. The 1D-FFT algorithm is then applied to each of the rows of the temporary array, and the result is a 64 × 64 complex array of real and imaginary Fourier components, R_{ik} and I_{jk}, where i and j are the row and column indices, respectively. The complex coefficients are then converted to polar form to produce 2-D amplitude and phase spectra A_{ij} and P_{ij}. Finally, the 2-D power spectral density $S(k_x, k_y)$ is calculated from the amplitude spectra by using

$$S(k_x, k_y) = \frac{D_x D_y \mid A_{ij} \mid^2}{MNH}, \tag{3}$$

where k_x, k_y are the x and y directed wavenumbers in cycles/m, D_x and D_y are the grid spacings in meters, $M, N = 64$ are the number of sample points, and H is the Hanning window correction factor that corrects for a reduction in PSD amplitudes caused by tapering of the data. Bendat and Piersol

(1971) and others show that for 1-D windows this factor is the ratio of the area under the square of the selected window to the area under the square of the equivalent uniform window. This result may be extended to two dimensions by setting the factor equal to the ratio of the volumes under the squares of the 2-D Hanning and uniform windows.

Spectrum Averaging

Averaging the individual power spectra according to the procedure of Welch (1967) produces a smooth spectrum and reduces random error in the spectral estimate. The normalized mean-square error E for a spectral estimate is given by

$$E^2 = E_r^2 + E_b^2 , \tag{4}$$

where E_r^2= (number of areas averaged)$^{-1}$ a random term and E_b is a bias term that is proportional to the resolution bandwidth of the spectral estimation process and the second derivative of the process within the band selected. If a red noise process is assumed, the bias error may be considered negligible and the fractional error for the average of n subareas is given by

$$E \sim (n)^{-\frac{1}{2}} . \tag{5}$$

For a random error of $<10\%$, at least 100 areas must be averaged. In this study, 170 spectra are included in the ensemble average, to produce a random error $\sim 7.7\%$.

CHARACTERISTICS OF THE SPECTRA OF SEAMOUNT ROUGHNESS

Nature of the Individual Power Spectra

Two-dimensional power spectral density (2D-PSD) estimates were computed for each of the 170 areas of Fig. 7 by using the procedures outlined in the discussion on data processing. The 2D-PSD estimates provide information on the sea floor roughness in terms of the energy content for a given wavelength or wavenumber and the angular variation of that energy. Based on the previous discussion, the spectra of this report present the energy in the residual bathymetry over the wavelength range of 1600 to 200 m. As an example of a typical result for the Apuupuu Seamount, Fig. 8 presents a perspective plot of the residual (plane removed) topography for one of the seamount subareas and its corresponding 2D-PSD. The horizontal axis of the plot is the wavenumber in the x or cross-slope direction, and the vertical axis is the wavenumber component in the y or upslope/downslope direction of the local bathymetry. The information plotted are 5 dB contours of the log magnitude of the 2D-PSD or power-spectrum level (SL) given by

$$SL\ (k_x, k_y) = 10 \log \left[\frac{S(k_x, k_y)}{\text{PSD - ref}} \right] \text{ dB} , \tag{6}$$

where PSD-ref = 1 m (cycles/m) is a normalizing factor to make the term in brackets unitless. The most prominent feature of Fig. 8 is a valley or trough-like feature running from the lower left to the upper right of the area. This feature in the bathymetry is reflected in the corresponding 2D-PSD as a distinct anisotropy throughout the wavenumber band in a direction normal to the axis of the trough. This anisotropy occurs because the trough represents an abrupt bathymetric discontinuity and thus has significant "wideband" energy for directions that cross the discontinuity. Figure 9 shows another 1600 m subarea of residual seamount topography. This subarea has a feature that approximates a wavetrain along the diagonal from the lower left to the upper right. The corresponding 2D-PSD again exhibits a strong anisotropy in a direction normal to the crest of the wavetrain, indicating significant spectral "energy" in that direction. Note, however, that the anisotropy does not extend throughout the full wavenumber band displayed, a result of the narrowband nature of a wavetrain. The contours near the origin and those at the higher wavenumbers are approximately circular. This indicates that at these

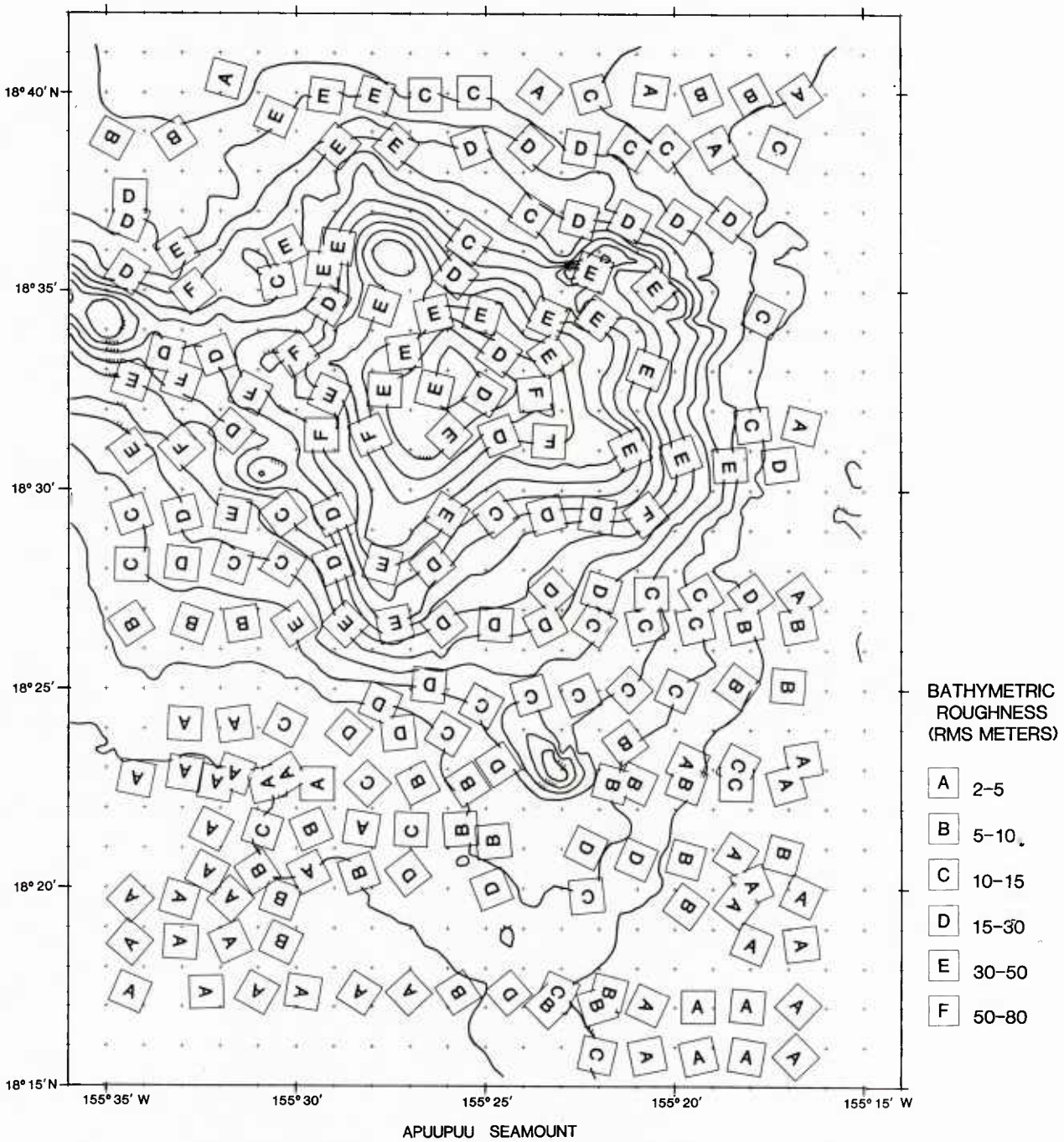

Fig. 7 — Location, orientation, and roughness range of the samples of bottom topography for the Apuupuu Seamount

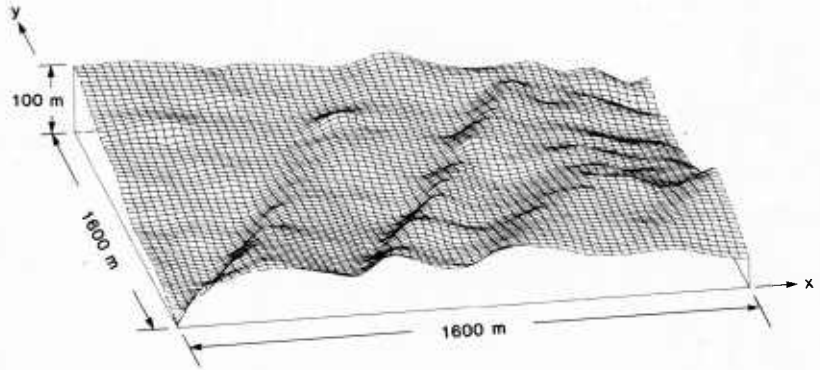

RESIDUAL BATHYMETRY SWATH

(a)

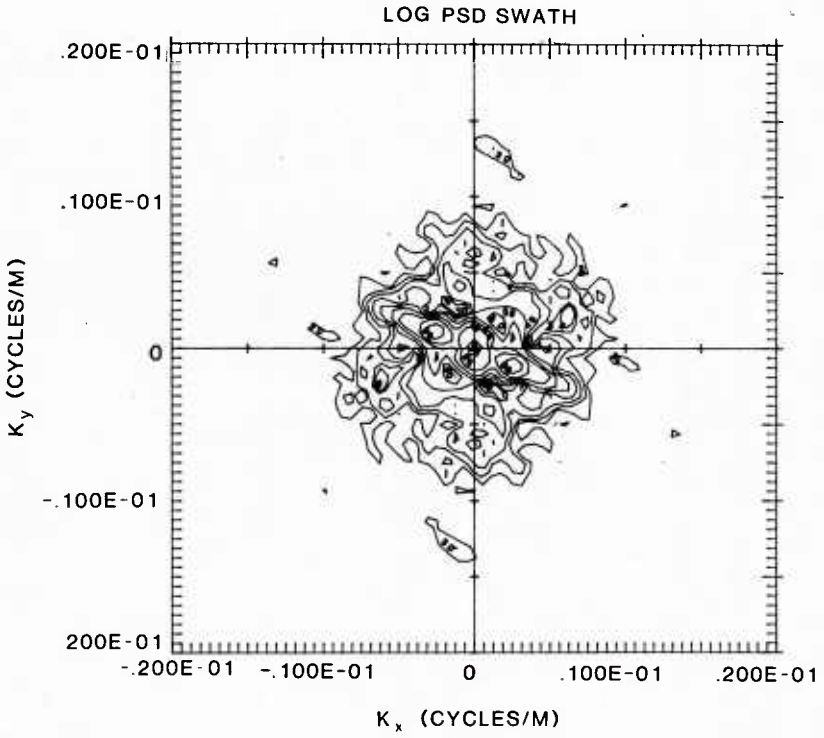

(b)

Fig. 8 — Example of residual seamount topography with a pronounced wave-like structure and its corresponding two-dimensional power spectrum

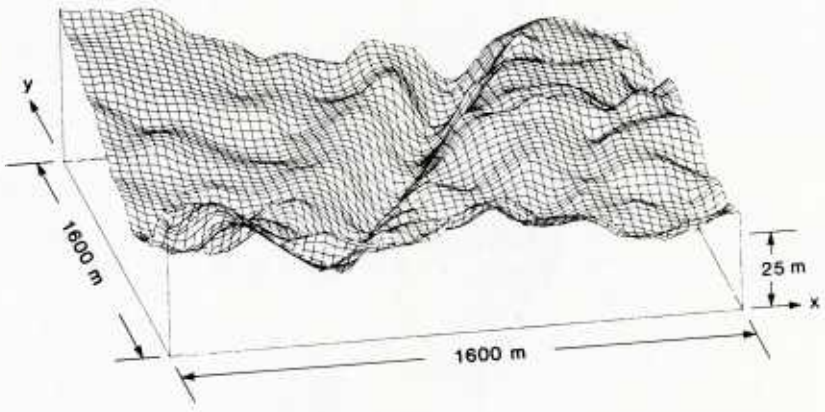

RESIDUAL BATHYMETRY SWATH

(a)

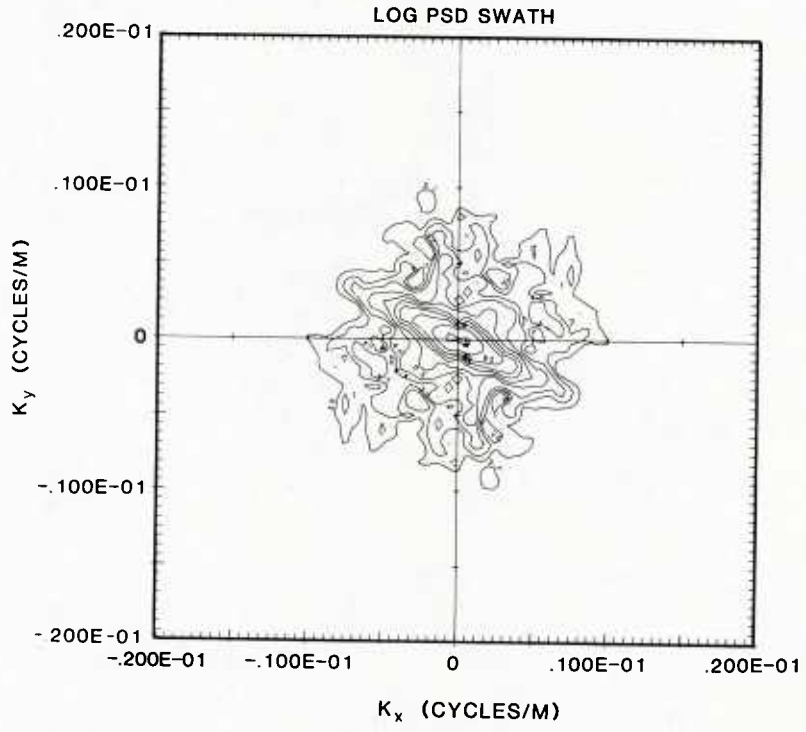

(b)

Fig. 9 — Residual topography exhibiting a trough-like feature and its corresponding two-dimensional power spectrum

feature scales the spectral energy distribution is essentially isotropic. A third example of residual topography and its corresponding spectrum is shown in Fig. 10 and represents topography that has strong anisotropy in the very long wavelengths, as exhibited by the peaks in the spectrum near the origin and by the rolling "hill-like" nature of the terrain. These examples illustrate the complex nature of the bottom topography and the utility of the 2D-PSD in describing both the qualitative nature and directional orientation of its features.

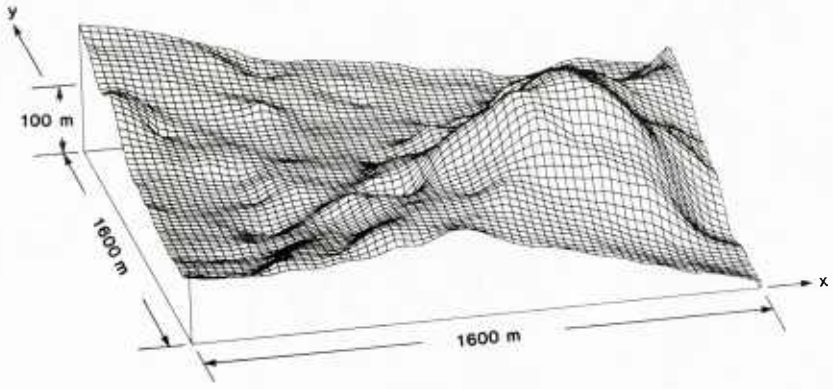

(a)

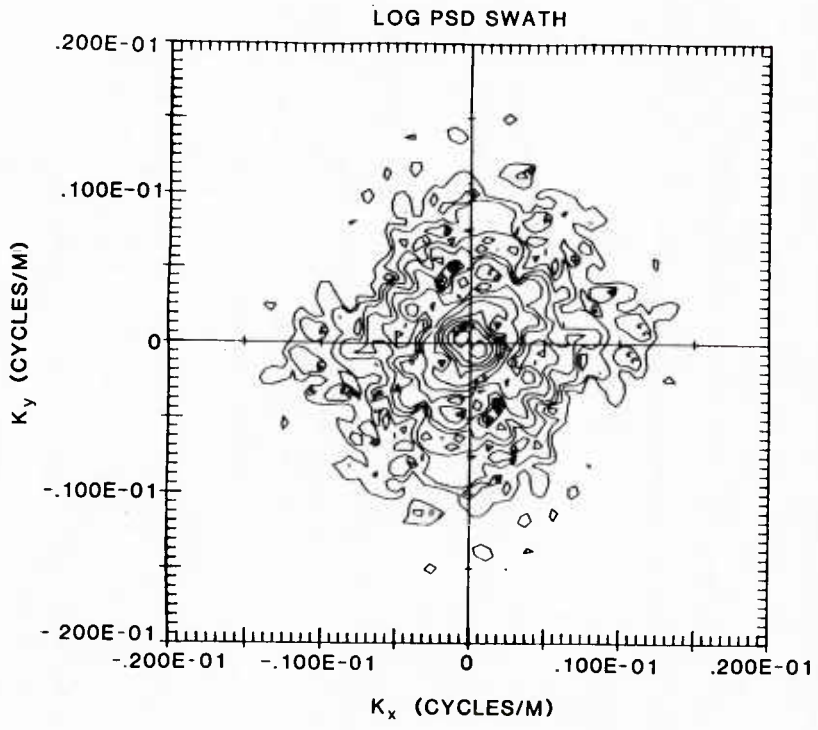

(b)

Fig. 10 — A third example of residual seamount topography showing longer wavelength, hill-like features, and the corresponding power spectrum

The Ensemble Average Spectrum and its Functional Representation

Individual spectra, while providing insight into the spatial variability of the local bathymetry, are not statistically significant for describing the bathymetry as a stochastic process. It is necessary to construct an ensemble average over many samples to reduce the variance of the estimate and, thereby,

achieve a spectral characterization that describes statistically significant aspects of the process. The spectra are averaged in a manner similar to the procedure of Welch (1967). Figure 11 presents the ensemble average of the 170 spectra for the Apuupuu Seamount. As might be expected, the averaging process produces a relatively smooth spectrum in comparison to the individual spectra discussed earlier that contain dramatic variations associated with the individual bottom samples.

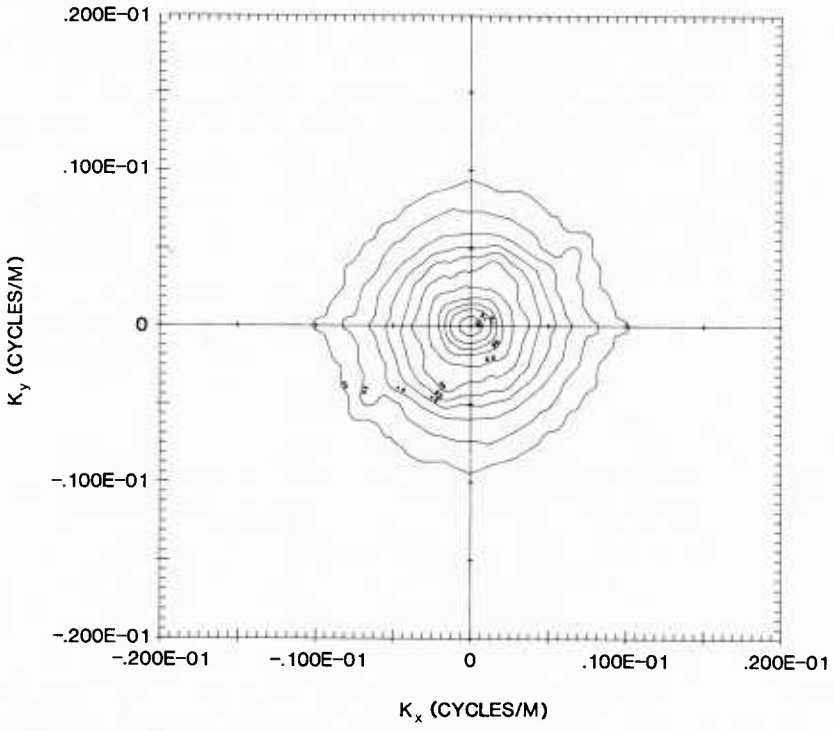

Fig. 11 — Ensemble average spectrum for Apuupuu Seamount

The most significant aspect of the average spectrum is that it suggests that the bottom topography in the waveband being considered is of a "red" noise character. This topography exhibits a general decrease of spectral energy with increasing wavenumber and with no isolated peaks, as would be the case for a narrowband process or a process with a strong sinusoidal component. This qualitative aspect of the spectrum is in agreement with the 1-D results of other investigators (see, for example, Bell, 1979 and Berkson and Matthews, 1984) for a variety of physiographic regimes. Figure 11 shows that the contours of equal energy are approximately circular from the origin out to a wavelength of 400 m. At wavelengths in the band from 500 to 200 m, the contours show a deviation from circular and exhibit an anisotropy in the downslope direction of $\sim 70°$. Spectral values for wavelengths shorter than 200 m occur as a result of oversampling the data; they are highly dependent on the nature of the interpolation process and are not discussed further. An important implication of the form of the 2-D spectrum shown in Fig. 11 is that there is a strong isotropic component to the process.

A functional representation of the average spectrum can be constructed easily because of the approximately monotone behavior of the spectrum along any ray emanating from the origin of the spectral plane. We seek a directional power law relationship of the form

$$S(k_x, k_y) = S_0(\theta)\,(k/k_0)^{\alpha(\theta)}\,, \tag{7}$$

where k, θ are polar coordinates in the spectral plane measured counterclockwise from the positive k_x axis, and k_o is a reference wavenumber. Note that the logarithm of Eq. (7) yields

$$\log\left[S(k_x, k_y)\right] = \log\left[S_0(\theta)\right] + \alpha(\theta)\ \log\left[k/k_0\right]. \tag{8}$$

Equation (8) represents a linear function with parameters being the spectral slope parameter α and a spectral intercept log $[S_o]$. Both may vary as a function of azimuthal angle θ in the spectral plane. This is clearly a generalization of power law representations used for 1-D data and allows useful quantitative summaries of the spectral behavior to be made. The term S_o is the spectral energy density at k_o and may be considered an energy scale factor for the spectrum. The reference wavenumber k_o was selected to be the average log wavenumber in the band of interest. Note that the spectral slope parameter α provides a measure of the relative contributions of the long and short wavelength content of the residual bathymetry. Bathymetry with large (negative) spectral slopes exhibits relatively higher energy at the longer wavelengths and is characterized as "hilly" features or features with large-scale curvature. Bathymetry with small spectral slopes is characterized as having a more balanced, or white-noise type, wavelength content. The combination of the spectral slope parameter α and the energy scale factor S_o makes it possible to differentiate between bathymetry that has the same relative wavenumber composition but different scales of total spectral energy content. The two parameters in the power law models of Eqs. (7) and (8) thus have the advantage of providing information about the relative size and wavenumber content of the bathymetry and, when specified as a function of azimuthal angle θ, provide a very compact way of specifying the spectral content of the bottom variability as a function of direction. The functional representation in Eq. (8) is also useful because it allows comparisons to be made with the results of other analyses and, if necessary, provides a basis for extrapolating the results to shorter wavelengths.

A rather general method of obtaining parameter values for the power law model can now be outlined. If behavior along a radial direction is of interest, we select a sector containing the desired direction. All spectral values in the sector are, in effect, rotated to the common direction simply by regarding each spectral value $S(k_x, k_y)$ as applying to the direction with a wavenumber of magnitude k where

$$k = (k_x^2 + k_y^2)^{\frac{1}{2}} . \tag{9}$$

The logarithm of the spectral values are then fit by a linear function in a least-squares sense. This procedure yields the parameters of the power law model. It is a flexible procedure because the angular span of the sector can be freely specified, depending on how accurately the angular representation is to be represented.

An example of the curve fit is shown in Fig. 12 for a 22.5° sector centered on the k_x axis for the 2-D spectrum of Fig. 11. A linear function of the form of Eq. (10) with $\alpha = -4.8$ and log $(S_o) = 5.85$ is shown to provide a reasonable fit to the data in the range of wavenumbers from 0.001 to 0.005 cycles/m. The result of using 22.5° sectors to represent the angular variation of the spectrum is shown in Fig. 13. It is only necessary to present the results for two quadrants of the spectrum because of the radial symmetry of the spectral values. The results provide some additional insight into how the wavelength content of the residual bathymetry varies as a function of direction. Figure 13 shows that the spectral slope varies as a function of angle by ~25% from the angular mean of −4.4. The steepest spectral slope ($\alpha = -4.8$) occurs in the cross-slope directions ($\theta = 0°, 180°$), while the most gradual slope ($\alpha = -3.5$) occurs at an angle of ~67.5°. The corresponding plot of S_o as a function of azimuth mirrors this anisotropy because the maximum in S_o also occurs at 67.5°. These results indicate that the shorter wavelength content of the seamount residual bathymetry is more significant in the upslope/downslope directions, while in the cross-slope directions the longer wavelength content predominates. The range of the results suggest, however, that to a first order the spectrum may be considered to be isotropic, that is, anisotropy appears to be a second-order effect for the Apuupuu Seamount in the waveband being considered.

An isotropic power law model may be fit to the spectrum by applying the above procedure where the sector is taken to have an angular extent of 180°. The result of the procedure is to obtain a functional representation independent of angle with $S_o = 7.8 \times 10^5 \text{m}^2/(\text{cycles/m})$, $\alpha = -4.54$, and the reference wavenumber $k_o = 0.00029$ cycles/m is the same as that used earlier. Thus the 2-D spectrum is assumed to depend only on the magnitude of the wavenumber. It is interesting to compare the values of the parameters for the isotropic approximation to the earlier case in which 22.5° sectors are used.

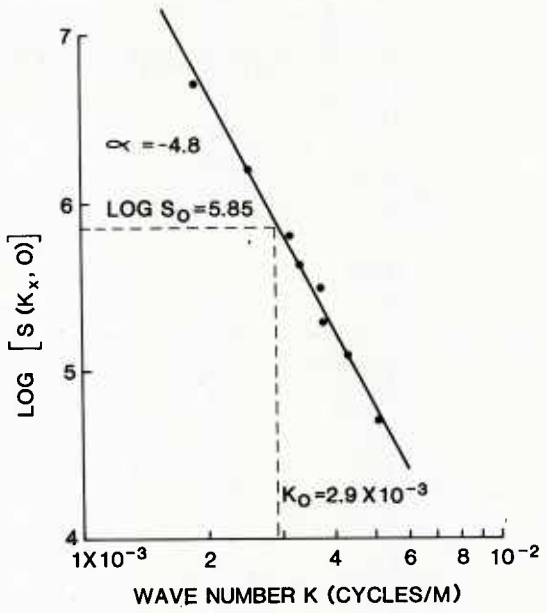

Fig. 12 — Plot of spectral data points along x-axis of two-dimensional spectra and least-squares estimate of power law model

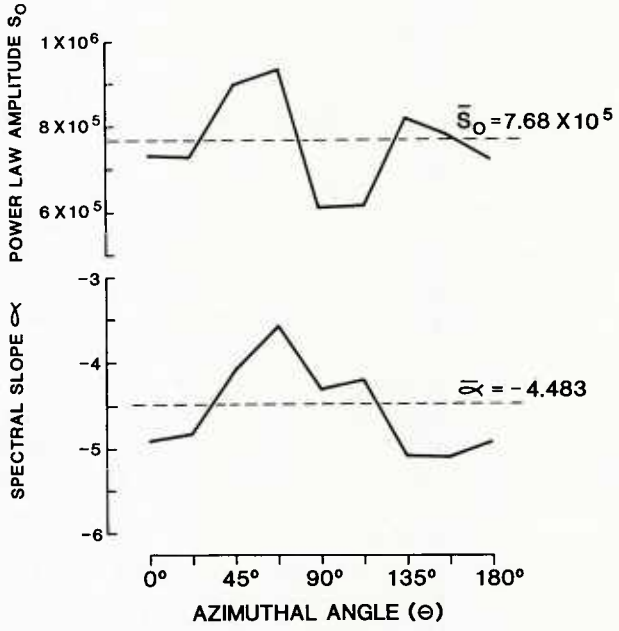

Fig. 13 — Plot showing variations as a function of direction of spectral slope and power law amplitude for Apuupuu Seamount

The values of α and $\log(S_o)$ are similar to the averages of the values obtained when 22.5° sectors are used, as can be seen in Fig. 13. This provides some quantitative justification to the statement that the 2-D spectrum simply shows fluctuations about an isotropic model.

Reducing the Two-Dimensional Spectrum to One-Dimensional Spectra

An important aspect of the 2-D spectral analysis is to investigate the implications for 1-D spectra. This is particularly relevant for ocean bottom topography because previous statistical studies have been presented in the form of 1-D spectral estimates. Unfortunately, in the absence of a condition of isotropy it is difficult to directly compare 2-D spectral results with spectra generated by 1-D sampling of an inherently 2-D process. The form of the 1-D spectra will be misleading, since at a given wavenumber k, energy will appear that corresponds to all wavenumber vectors whose projection in the direction of the 1-D track have a magnitude equal to k. Thus, at lower values of wavenumber, the 1-D spectrum receives contributions from wavenumbers of much higher magnitude. In this sense, the 1-D spectra generated from single-track samples of an anisotropic process are considered to be "aliased" spectra. They must be interpreted with some caution when statements are made about the full 2-D spectrum. We first derive 1-D spectra for the cross-slope and downslope directions. This is simply done by integrating over the full 2-D spectrum. Thus, the 1-D spectrum for the cross-slope direction is given by

$$S(k_x) = \int_{-\infty}^{\infty} S(k_x, k_y)\, dk_y \,. \tag{10}$$

Note that the mean-square residual elevation is given by

$$\eta^2 = \int_{-\infty}^{\infty} \int_{-\infty}^{\infty} S(k_x, k_y)\, dk_x\, dk_y \tag{11}$$

and can be written as

$$\eta^2 = \int_{-\infty}^{\infty} S(k_x)\, dk_x \tag{12}$$

by using Eq. (10). This indicates that $S(k_x)$ gives the energy density of the contribution to the mean-square residual elevation arising from a wavenumber k_x. A formula similar to Eq. (10) relates $S(k_y)$ to the 2-D spectrum $S(k_x, k_y)$. When the integrations are performed on the estimate of the 2-D spectrum shown in Fig. 11, we obtain estimates of the 1-D spectra for the cross-slope and upslope/downslope directions. Figure 14 shows the 1-D spectra generated in this manner for the Apuupuu Seamount. These spectra represent estimates of 1-D spectra generated by sampling the residual seamount bathymetry in the cross-slope and downslope directions. Also shown in the figure are power law approximations to the 1-D spectra obtained by determining least-square fits to the plotted spectral values. The results indicate a spectral slope of −3.9 for the cross−slope direction and −2.9 for the downslope direction.

It is also of interest to determine the 1-D spectrum that would be associated with an isotropic approximation to the 2-D spectrum of Fig. 11. We indicated earlier that $S(k_x, k_y)$ may be approximately represented in an isotropic form, that is, dependent only on k. The isotropic spectrum is then given by

$$S(k) = 2\pi k\, S(k_x, k_y) \tag{13}$$

where it is intended that the isotropic approximation of $S(k_x,k_y)$ is used in Eq. (13). The spectrum S(k) is often refered to as a scalar wavenumber spectrum. An important aspect of an isotropic spectrum for a 2-D process is that all 1-D spectra obtained from it are the same. This is because all 1-D samples

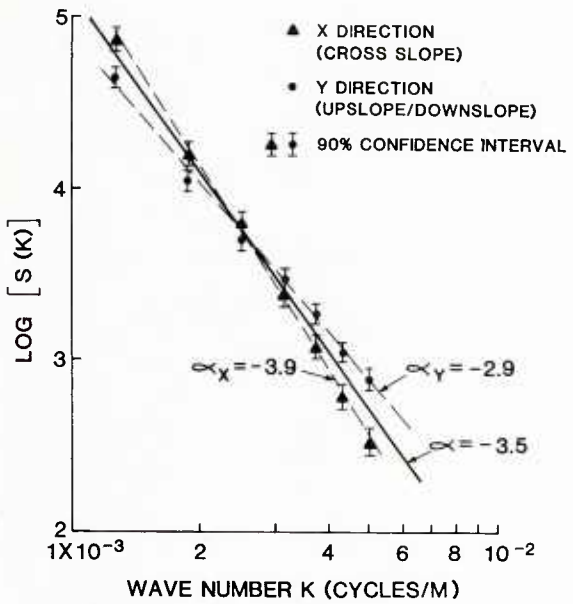

Fig. 14 — Plot showing x-directed, y-directed, and isotropic estimates of one-directional spectra computed from the ensemble average spectrum for Apuupuu Seamount

of the process effectively see the same statistical behavior. The 1-D spectrum associated with the isotropic 2-D spectrum $S(k)$ is easily found to be

$$S(k') = \pi^{-1} \int_{k'}^{\infty} S(k)\ (k^2 - k'^2)^{-\frac{1}{2}} dk\ , \tag{14}$$

where k' represents a wavenumber for the 1-D record and can be taken as equal to k_x or k_y. In terms of the 2-D spectral slope parameter of Eq. (7), Eq. (10) indicates that the scalar wavenumber spectrum has a spectral slope of $+1$. It may also be shown from the form of Eq. (14) that the spectral slope for $S(k')$ is also $+1$ under these circumstances. We earlier found that $S(k_x, k_y)$ may be approximated by an isotropic form with a spectral slope of -4.5. This gives a 1-D spectrum with a spectral slope of -3.5. The 1-D spectrum associated with the approximation of regarding the 2-D spectrum as isotropic is plotted as a solid curve in Fig. 14 and appears to represent a reasonable compromise between the spectral results for the cross-slope and downslope directions.

The results shown in Fig. 14 have important implications for the discussion of isotropy of the 2-D spectrum, which is a principal theme of this report. In our discussion of the 2-D spectrum, the results suggest that the anisotropy present appears to be aligned relative to the cross-slope and downslope directions. This motivates the use of the 1-D spectra for the x and y directions as an effective means of discussing the anisotropy. The results for the cross-slope and downslope spectra are shown in Fig. 14, together with the confidence interval at the 90% level. We note that if the residual bottom topography is isotropic, the cross-slope and downslope spectra would agree with one another within the limits imposed by statistical uncertainty. In particular, we expect the spectral estimates for the two spectra to lie within one confidence interval of one another. It is clear from Fig. 11 that, although the cross-slope and downslope spectra are close to one another, there is a distinct pattern to their deviations that lies outside the limits of the confidence interval. We conclude that the process must be regarded as inherently anisotropic but with a strong isotropic component. This is suggested by the comparison in Fig. 14 of the cross-slope and downslope spectra with the 1-D spectrum derived from the isotropic approximation.

A particular implication of the anisotropy is that it confirms the need to align the bottom areas to a common reference that is appropriate to the process being studied. A more general statement of this,

applicable to other spectral analyses of bottom topography, is that it is necessary to consider sampling geometry relative to the process.

The nature of the anisotropy indicates that spectral energy will be oriented more in the cross-slope direction at lower wavenumbers (longer wavelengths) and more in the downslope direction at higher wavenumbers (shorter wavelengths). It is possible to give a specific quantitative meaning to the previous statement by using the wavenumber k^* defined by the intersection of the cross-slope and downslope spectra as a "characteristic" spatial scale of the anisotropic process. The value of $k^* = 0.0025$ cycles/m establishes 400 m as the associated characteristic wavelength of the process.

Since the 2-D spectral analysis carried out here applies to a fairly restricted band of wavenumbers, it is tempting to ask what the implications are if the results are extrapolated outside the band. This must be done with some care. It is essentially an illegitimate operation to extrapolate the spectral behavior to lower wavelengths because it implies that we are examining spectral components whose wavelengths are much larger than the dimensions of the subarea used in the analysis. The dimension of the subarea is also that over which a mean plane is used to determine a downslope orientation direction. Consequently, it is possible that a different mean plane as well as reference direction is needed for an analysis of the lower wavenumbers. We can, however, examine the implications of extrapolating the spectral behavior to higher wavenumbers since this does not violate any inherent conditions of the spectral analysis.

The main implication of Fig. 14 for anisotropy of the process is that the downslope spectrum contains an increasing amount of energy relative to the spectrum in the cross-slope direction for wavenumbers larger than the critical wavenumber. This statement is based on the assumption that the spectral behavior shown in Fig. 14 can be extrapolated to a higher wavenumber regime. If true, it would mean that the higher wavenumber components tend to have an orientation aligned in the downslope direction on the Apuupuu Seamount. The physical context of this extrapolated behavior must be interpreted carefully because downslope and cross-slope have been defined in terms of the local properties of the larger scale aspects of the seamount. In particular, recall that a mean plane was used to define the downslope direction. For the Apuupuu Seamount, one of the large-scale aspects of the topography noted previously was a radial ridge structure. Subareas located on one of the radial ridge arms then have a downslope direction that tends to be oriented perpendicular to the direction of the radial ridge. Such aspects of the seamount topography must be remembered when relating the results of the spectral analysis to the seamount, viewed in its entirety.

It is interesting to relate our results to other studies of the spectral properties of seamount topography. The only pertinent results appear to be due to Berkson and Matthews (1984) who analyzed 1-D track samples of a number of bottom provinces, including a seamount. The analysis was apparently made under an assumption that the process is isotropic, and it is difficult to assess what effect the failure of a condition of isotropy would have on their spectral results. Although our results indicate an anisotropic structure to residual topography on a seamount, it can be argued that the 2-D spectrum has a strong isotropic component, at least for the band considered. On this basis, the results for Apuupuu suggest that 1-D samples of the residual topography with random azimuthal orientations would yield a spectrum with a spectral slope of ~ -3.5. This result should be compared to a value of -2.2 given by Berkson and Matthews (1984) for a seamount in the Atlantic over a comparable wavenumber band.

We have, then, a distinct difference with the Berkson and Matthews result for the spectral behavior of seamount topography that indicates that a single spectral model with fixed parameters does not describe the statistical behavior of residual topography on a seamount. An important implication of this is that the spectrum may be sensitive to important physical aspects of the seamount, such as geological age or other characteristics related to its formation and evolution. However, the full investigation of this implication requires a detailed study of several seamounts that adequately represent the wide range of possible behavior.

CONCLUDING REMARKS

The central motivation of this report was to investigate the 2-D spectrum of residual topography as a useful statistical property of the bottom topography. The analysis is confined to numerous samples of bottom topography from the Apuupuu Seamount, although the general procedures and considerations are equally applicable to other ocean bottom provinces. The general importance of the results is that they provide the first 2-D spectrum of bottom topography derived from 2-D bathymetric data. This is made possible by extensive measurements performed by a multibeam bathymetric mapping system and provides detailed sampling of the ocean bottom topography over a 2-D spatial grid.

The topography of a Pacific seamount, Apuupuu, is considered in detail in this report. The topography of a seamount is regarded as being a stochastic process that "evolves" in two spatial dimensions, and a statistical analysis of the roughness of the Apuupuu Seamount was based on 170 2-D samples of bottom topography. A particular issue in the analysis of such processes involves the anisotropy of the process or the existence of a preferred direction on which the statistical properties will depend. This issue either does not arise in 1-D studies or is typically ignored in analyses of 1-D bottom topography. The analysis carried out here is based on selecting the local downslope direction as a means of orienting all the topographic samples to a common reference direction. This allows the statistical analysis to focus on the dependence of the shorter scale variability on the larger scale features of the seamount, such as radial ridges and rifts. The 2-D power spectral density is determined by ensemble averaging over the 170 sample spectra and shown to possess some interesting properties. Although the spectrum indicates a directional dependence, the most prominent characteristic is that it contains a strong isotropic component that can be represented as a power law dependence with a spectral slope of -4.5. The anisotropy present appears to be a second-order effect. The anisotropy can be further characterized by examining the 1-D spectra for the downslope and cross-slope directions. These spectra may also be represented as power law behavior with spectral slopes of -2.9 and -3.9 for the downslope and cross-slope directions, respectively. An important aspect of the 1-D spectra is that they establish a characteristic scale of 400 m such that for topographic variability at a horizontal scale shorter than 400 m the spectral components tend to be oriented in the downslope direction. This is perhaps the simplest statement that can be made for the statistical behavior of the roughness of the Apuupuu Seamount.

The question of whether similar properties apply to other seamounts must await further studies of seamount roughness. However, the difference between the spectral slope found here and that found in other studies that considered spectral analysis of seamount topography (Berkson and Matthews, 1984) suggests the possibility that the spectral properties of roughness may be related to characteristics associated with the formation and evolution of the seamount. Should this prove the case, it would underscore the importance of the spectrum as a useful quantitative characteristic for the classification and investigation of ocean bottom topography.

REFERENCES

Akal, T. and J. Hovem (1978). "Two-dimensional Space Series Analysis for Sea-Floor Roughness," *Marine Geotechnology*, **3** (2), 171-182.

Bell, T.H., Jr., (1975). "Statistical Features of Sea-Floor Topography," *Deep-Sea Res.* **22**, 883-892.

Bell, T.H., Jr., (1979) "Mesoscale Sea Floor Roughness," *Deep-Sea Res.* **26A** 65-76.

Bendat, J.S. and A.G. Piersol, (1971) *Random Data: Analysis and Measurement Procedures* (Wiley, New York).

Berkson, J.M. and J.E. Matthews (1984), "Statistical Characterization of Seafloor Roughness," *IEEE J. Oceanic Eng.* **OE-9** (1), 48-51.

Brown, S.R. and Scholz (1984), "Broad Bandwidth Study of the Topography of Natural Rock Surfaces," presented at the 1984 Fall Meeting of the Am. Geophys. Union.

Frederiksen, P. and O. Jacobi (1981), "Terrain Classification by Fourier Analysis," *Proc. Am. Soc. Photogrammetry Annual Meeting*, 267-284.

Glenn, M.F., (1970), "Introducing an Operational Multibeam Array Sonar," *International Hydrographic Rev.* **47**, 35-39.

Harris, F.J. (1978), "On the Use of Windows for Harmonic Analysis with the Discrete Fourier Transform," *Proc. IEEE* **66** (1), 51-83.

Kinsman, B. (1965), *Wind Waves* (Prentice-Hall, Englewood Cliffs, N.J.).

McDonald, M.F. and E. J. Katz (1969), "Quantitative Method for Describing the Regional Topography of the Ocean Floor," *J. Geophys. Res.* **74**, 2597-2607.

Neidell, N.S. (1960), "Spectral Studies of Marine Geophysical Profiles," *Geophysics* **31**, 122-134.

Phillips, J.D. and H. S. Fleming (1977), "Multi-beam Sonar Study of the Mid-Atlantic Ridge Rift Valley," *Geol. Soc. Am. Mapping and Charting Series* **MC-19**, 1-24.

Robinson, E.A. and M. T. Silvia (1981), *Digital Foundations of Time Series Analysis*, (Holden-Day, San Francisco), Vol. 2.

Swain, C.J. "A Fortran IV Program for Interpolating Irregularly Spaced Data Using the Difference Equations for Minimum Curvature," *Computers and Geosciences,* **1**, 231-240.

Thomson, D.J., M.F. Robbins, C.G. Maclennan, and L.J. Lanzerotti (1976), "Spectral and Windowing Techniques in Power Spectral Analyses of Geomagnetic Data," *Phys. Earth and Planetary Interiors* **12**, 217-231.

Tucker, D.G. and J. G. Henderson (1960), "Automatic Stabilization of Underwater Acoustic Beams Without Mechanical Motion of the Transducer," *Int. Hydrogr. Rev.* **37**, 69-78.

Vogt, P.R. and N. C. Smoot (1984), "The Geisha Guyots: Multibeam Bathymetry and Morphometric Interpretation", *J. Geophys. Res.* **89**, (B13), 11085-11107.

Welch, P.D. (1967), "The Use of Fast Fourier Transform for the Estimation of Power Spectra: A Method Based on Time Averaging over Short, Modified Periodograms," *IEEE Trans. Audio and Electroacoustics,* AU-15, 70-73.

Superintendent
Naval Postgraduate School
Attn: Technical Library
Monterey, CA 93940